NeuroImage: Clinical 18 (2018) 591–598

Contents lists available at ScienceDirect

NeuroImage: Clinical

journal homepage: www.elsevier.com/locate/ynicl

Gray matter changes in asymptomatic *C9orf72* and *GRN* mutation carriers

Karteek Popuri[a], Emma Dowds[b], Mirza Faisal Beg[a], Rakesh Balachandar[a], Mahadev Bhalla[a], Claudia Jacova[c], Adrienne Buller[a], Penny Slack[b], Pheth Sengdy[b], Rosa Rademakers[d], Dana Wittenberg[b], Howard H. Feldman[e], Ian R. Mackenzie[f], Ging-Yuek R. Hsiung[b,*]

[a] School of Engineering Science, Simon Fraser University, Canada
[b] Division of Neurology, Department of Medicine, University of British Columbia, Canada
[c] School of Professional Psychology, Pacific University, Hillsboro, OR, USA
[d] Department of Neuroscience, Mayo Clinic Jacksonville, FL, USA
[e] Department of Neurosciences, University of California San Diego, CA, USA
[f] Department of Pathology and Laboratory Medicine, University of British Columbia, Canada

ARTICLE INFO

Keywords:
Frontotemporal dementia
Magnetic resonance imaging
C9orf72 mutation
Granulin mutation
Cortical thickness
Subcortical volumes

ABSTRACT

Frontotemporal dementia (FTD) is a neurodegenerative disease with a strong genetic basis. Understanding the structural brain changes during pre-symptomatic stages may allow for earlier diagnosis of patients suffering from FTD; therefore, we investigated asymptomatic members of FTD families with mutations in *C9orf72* and granulin (*GRN*) genes. Clinically asymptomatic subjects from families with *C9orf72* mutation (15 mutation carriers, *C9orf72*+; and 23 non-carriers, *C9orf72*−) and *GRN* mutations (9 mutation carriers, *GRN*+; and 15 non-carriers, *GRN*−) underwent structural neuroimaging (MRI). Cortical thickness and subcortical gray matter volumes were calculated using FreeSurfer. Group differences were evaluated, correcting for age, sex and years to mean age of disease onset within the subject's family. Mean age of *C9orf72*+ and *C9orf72*− were 42.6 ± 11.3 and 49.7 ± 15.5 years, respectively; while *GRN*+ and *GRN*− groups were 50.1 ± 8.7 and 53.2 ± 11.2 years respectively. The *C9orf72*+ group exhibited cortical thinning in the temporal, parietal and frontal regions, as well as reduced volumes of bilateral thalamus and left caudate compared to the entire group of mutation non-carriers (NC: *C9orf72*− and *GRN*− combined). In contrast, the *GRN*+ group did not show any significant differences compared to NC. *C9orf72* mutation carriers demonstrate a pattern of reduced gray matter on MRI prior to symptom onset compared to *GRN* mutation carriers. These findings suggest that the preclinical course of FTD differs depending on the genetic basis and that the choice of neuroimaging biomarkers for FTD may need to take into account the specific genes involved in causing the disease.

1. Introduction

Frontotemporal Dementia (FTD) is a heterogeneous clinical syndrome characterized by progressive alterations in behavior, personality, language, and motor function (McKhann et al., 2001; Snowden et al., 2005). Approximately half of affected individuals have a positive family history, with alterations in three genes responsible for the majority of the inherited cases (Snowden et al., 2002; Seelaar et al., 2008; Feldman et al., 2003). Mutations in the gene encoding the microtubule associated protein tau (*MAPT*) are responsible for familial FTD associated with tau pathology, while mutations in the granulin (*GRN*) and chromosome 9 open reading frame 72 (*C9orf72*) genes cause FTD with transactive response DNA binding protein M_r 43 kDa (TDP-43) pathology (Snowden et al., 2002; Warren et al., 2013; Pan and Chen, 2013; Renton et al., 2011; Gijselinck et al., 2012; DeJesus-Hernandez et al., 2011; Baker et al., 2006; Cruts et al., 2006). Since each of these mutations cause an autosomal dominant inheritance with a high degree of penetrance, asymptomatic mutation carriers could be considered "preclinical" and are appropriate subjects for investigating the pre-symptomatic stages of FTD.

Studies that have investigated the structural brain changes in fully affected FTD patients with the *C9orf72* mutation have reported symmetric atrophy of frontal lobes, followed by temporal and parietal lobes (Boxer et al., 2011; Mahoney et al., 2012; Whitwell et al., 2012a; Sha et al., 2012). In contrast, symptomatic *GRN* mutation carriers have been reported to have asymmetric atrophy involving the left inferior frontal, temporal and parietal cortices (Mahoney et al., 2012; Whitwell et al., 2012a; Rohrer et al., 2010; Whitwell et al., 2009). Similar findings have

* Corresponding author at: Division of Neurology, Department of Medicine, University of British Columbia, S151 – 2211 Wesbrook Mall, Vancouver, BC V6T 2B5, Canada.
E-mail address: hsiung@mail.ubc.ca (G.-Y.R. Hsiung).

https://doi.org/10.1016/j.nicl.2018.02.017
Received 21 November 2017; Received in revised form 25 January 2018; Accepted 16 February 2018
Available online 17 February 2018

been reported in asymptomatic *GRN* mutation carriers, displaying asymmetric gray matter atrophy involving frontal, temporal and parietal lobes (Cruchaga et al., 2009; Pievani et al., 2014). A recent large scale study from the "Genetic Frontotemporal dementia Initiative (GENFI)" reported heterogeneous patterns of structural changes associated with *C9orf72* and *GRN* gene mutations in combined samples of symptomatic and asymptomatic subjects (Rohrer et al., 2015). The findings of the GENFI study suggest that structural brain changes could be detected many years prior to disease onset.

Most studies to date have employed symptomatic carriers or a combination of symptomatic and asymptomatic subjects to investigate the structural brain changes associated with *C9orf72* and *GRN* mutations (Mahoney et al., 2012; Whitwell et al., 2012a; Rohrer et al., 2010; Whitwell et al., 2009; Rohrer et al., 2015). As the aim of our study is to investigate brain changes prior to onset of clinical symptoms, we placed the focus on asymptomatic subjects in our current analysis. We hypothesize that *C9orf72* and *GRN* mutation carriers (*C9orf72*+ and *GRN*+, respectively) would exhibit regional atrophy compared to family members who do not carry the mutations (*C9orf72*− and *GRN*−) and that the patterns of atrophy would be different between the *C9orf72*+ and *GRN*+ groups.

2. Materials and methods

2.1. Subjects

Participants were recruited through the University of British Columbia (UBC) hospital clinic for Alzheimer's disease and related disorders. Each subject was a member of a family with autosomal dominant FTD caused by a mutation in either the *C9orf72* or *GRN* gene, and each was considered at risk for FTD by virtue of having an affected first-degree relative. All subjects underwent genetic analysis to establish whether they were carriers of their family's mutation; however, the subjects and the investigators performing the clinical assessments remained blinded to the genetic results. Some features of the cohort have been described previously (Jacova et al., 2013; Hallam et al., 2014). Participants underwent a detailed neurological examination and were screened for cognitive deficits with various scales including the mini mental state examination (MMSE) (Folstein et al., 1975; Folstein et al., 1983), Frontal Assessment Battery (FAB) (Dubois et al., 2000), and the Frontal Behavioral Inventory (FBI) (Kertesz et al., 2000). None of the subjects in the current analysis demonstrated any abnormal motor finding or reflexes, or any significant differences in the ALS motor scales. Patients who fulfilled the diagnostic criteria for possible or probable behavioral variant FTD (bvFTD) (Rascovsky et al., 2011), primary progressive aphasia (PPA) (Gorno-Tempini et al., 2011) or amyotrophic lateral sclerosis (ALS) (Brooks et al., 2000) were excluded. Participants who were free from neurological and clinical cognitive deficits and classified as being asymptomatic were included in the current analysis. Demographic information and family history were shown in Table 1. Years prior to expected disease onset was calculated by subtracting the subjects age from the mean age of disease onset in their respective family. The study was reviewed by institutional research ethics board, and written informed consent was obtained from the participants prior to data collection.

2.2. Genetic status

Genetic analysis was performed at the Mayo Clinic, Jacksonville, Florida, on DNA extracted from peripheral blood using standard protocols (DeJesus-Hernandez et al., 2011; Baker et al., 2006). Subjects were screened for the mutation known to cause FTD in their family and each was classified as being a mutation carrier (*C9orf72*+ or *GRN*+) or non-carrier (neither *C9orf72*− nor *GRN*−). All the *C9orf72*+ subjects in our cohort had repeat size in the clearly positive (> 100) range.

2.3. MRI image acquisition

All subjects underwent structural T1-weighted MRI scanning using a 1.5T GE Signa scanner. The MRI scans were 256 × 256 × 256 in resolution with isotropic 1 mm^3 voxels, and were acquired using the following parameters: Localizers (0:25 min): sagittal/coronal and axial, TR/TE = 5.4/1.6 ms, FOV = 22 cm, matrix size = 256 × 128; 3D T1-Fast Spoiled gradient echo IR Prepped (8:35 min): axial, TR/TE = 10.3/4.8 ms, inversion time = 450 ms, FOV = 25 cm, matrix size = 256 × 256, number of slices = 170 contiguous slices, slice thickness = 1 mm and flip angle = 8^o.

2.4. Cortical thickness and subcortical volume measurements

The T1 MRI images were processed using FreeSurfer neuroimage analysis suite (https://surfer.nmr.mgh.harvard.edu) to generate surface-based cortical thickness maps for each subject. FreeSurfer's cortical reconstruction pipeline (Dale et al., 1999; Fischl et al., 1999) first extracts and tessellates the outer pial (gray matter-cerebrospinal fluid boundary) and the inner white (gray-white matter boundary) surfaces of the cortical mantle. Afterwards, cortical thickness is computed at each vertex of the tessellation as the shortest distance between the pial and white matter surfaces (Fischl and Dale, 2000). The automatic cortical reconstruction outputs were passed through a rigorous manual quality control procedure to identify and correct for any errors according to the troubleshooting guidelines provided by FreeSurfer. To facilitate statistical group analysis, the cortical thickness surface maps for each subject were mapped into the standard MNI ICBM 152 nonlinear average T1 template space (Grabner et al., 2006) (http://nist.mni.mcgill.ca/?p=858) and smoothed using a 15 mm full width at half maximum Gaussian kernel. This resulted in cortical thickness maps defined on a common surface tessellation containing 297,800 vertices and 64 labeled cortical regions of interest. Moreover, the volumetric segmentation pipeline (Fischl et al., 2002) in FreeSurfer was used to extract the volumes of the deep subcortical gray matter structures. Further, the cerebellar sub-region volumes were calculated by transferring the cerebellar sub-region labels from the SUIT atlas [cite Diedrichsen et al., 2009 and 2011] onto the subject's MRI using the large deformation diffeomorphic metric mapping (LDDMM) non-rigid registration method [cite: Beg et al., 2005]. The subcortical and cerebellar sub-region volumes were normalized using the intracranial volume (ICV) to correct for the brain size of the subject.

2.5. Statistical analysis

Group-wise comparison of the clinical and demographic variables were performed using the MATLAB 2016b (MathWorks, Inc., Natick, MA) numerical computing environment. Normality of the data was verified using Anderson-Darling test. Group difference was performed using independent *t*-test for normally distributed data, else the Wilcoxon rank sum test was used. Chi-square test was used for comparing the group differences in the distribution of categorical variables (sex). Results were considered statistically significant at p values < 0.05.

Vertex-wise group differences among the generated cortical thickness surface maps were explored using the SurfStat toolbox (www.math.mcgill.ca/keith/surfstat/) for MATLAB. A generalized linear model (GLM) approach was performed controlling for the effects of age, sex, and years prior to mean age of illness onset. The cluster significance threshold was set at $p < 0.05$, using random field theory (RFT) correction (Chung et al., 2010) for multiple comparisons, and only significant clusters consisting of > 100 vertices were reported. Similarly, GLM analysis was performed to evaluate the group differences in ICV normalized subcortical volumes correcting for the influences of age, sex and years prior to mean age of illness onset. Group wise comparisons were made between each of the carrier groups

Table 1
Summary of demographic and clinical features of the subjects. Maximum score is 30 for mini mental state exam (MMSE), 18 for the frontal assessment battery (FAB), and 72 for the frontal behavioral inventory (FBI). The values are reported as mean (std.). NC (non-carriers): *C9orf72*− and *GRN*− combined.

	C9orf72+	*C9orf72*−	*GRN*+	*GRN*−	NC	p^{*}	p^{**}
Sample size (n)	15	23	9	15	37	–	–
Age (years)	42.6 (11.3)	49.7 (15.5)	50.1 (8.7)	53.2 (11.2)	51.5 (13.9)	0.0227	0.7127
Sex (Male: Female)	8:7	13:10	1:8	7:8	19:18	0.8969	0.029
Handedness (Right: Left)	12:3	22:1	9:0	14:1	35:2	0.1058	0.4757
Education (years)	14.0 (3.3)	13.9 (2.9)	13.1 (2.9)	12.9 (2.3)	13.5 (2.7)	0.4117[#]	0.8288[#]
MMSE	29.5 (0.74)	29.04 (1.07)	29.3 (1)	29.2 (1.08)	29.1 (1.07)	0.1581[#]	0.5111[#]
FAB	17.1 (1.7)	16.09 (2.2)	16.6 (1.4)	17.4 (1.06)	16.6 (1.9)	0.1443[#]	0.5889[#]
FBI	0.73 (1.4)	0.39 (0.94)	0.67 (1.1)	0.67 (1.8)	0.51 (1.4)	0.6317[#]	0.4585[#]
Mean age (years) of onset in family	56.3 (7.9)	56.7 (6.6)	58 (3)	58.7 (3.2)	57.6 (5.6)	0.6108[#]	0.9433[#]
Years prior to mean age of illness onset	13.7 (11.2)	7 (14.4)	7.89 (8.9)	5.47 (10.03)	6.1 (12.8)	0.0433	0.6306

[*] *C9orf72*+ versus NC.
[**] *GRN*+ versus NC.
[#] Data did not follow normal distribution, hence non-parametric test (Wilcoxon rank sum) was employed.

against all mutation non-carriers (*C9orf72*− combined with *GRN*−, NC).

3. Results

3.1. Demographic and clinical data

Demographic and clinical information is provided in Table 1. Comparison between the *C9orf72*+ and NC revealed that *C9orf72* carriers are significantly younger and were also significantly further from the mean age of illness onset in their families. The *GRN*+ versus NC comparison showed significantly more females in the *GRN*+ group. Majority of the participants were right handed (only 5 left handed subjects were present), and no significant differences were observed in the handedness between mutation carriers and NC. Disease specific FAB and FBI assessments did not reveal any significant differences in the cognitive status between mutation carriers and NC.

3.2. Cortical thickness difference between groups

The *C9orf72*+ subjects demonstrated significant reductions in cortical thickness in certain regions of the brain compared to the NC group (Fig. 1 and Table 2). The affected areas involved both cerebral hemispheres in a somewhat asymmetric fashion and included select regions in the left frontal, left parietal, left occipital, left cingulate, right temporal and right parietal lobes. In contrast, the *GRN*+ subjects did not show any significant gray matter changes compared to the NC subjects, although visual inspection of the cortical thickness *z*-scores suggests quite a degree of variability and heterogeneity within the *GRN*+ group (Fig. 2).

3.3. Subcortical volume difference between the groups

The *C9orf72*+ subjects also exhibited significant reduction in the volumes of bilateral thalamus and left caudate volumes compared to the NC subjects (Table 3 and Fig. 3). The *GRN*+ subjects did not differ significantly in subcortical volumes compared to the *GRN*− subjects or NC group.

3.4. Cerebellar volume difference between the groups

We have also examined the cerebellar sub-region volumes, but no significant differences were observed between the mutation carriers (*C9orf72*+ and *GRN*+) and the NC (see Supplemental Table S1 and Fig. S1).

4. Discussion

In this study, we investigated the influences of *C9orf72* and *GRN* mutations on cortical thickness and subcortical gray matter volumes in asymptomatic members of FTD families. Our findings demonstrate discordant patterns of structural changes between our subjects with these two mutations. The *C9orf72*+ subjects demonstrated patterns of reduced cortical thickness and reduced subcortical volumes; whereas, the *GRN*+ subjects showed no significant cortical or subcortical gray matter atrophy. Furthermore, *C9orf72*+ subjects exhibited reduced subcortical volumes compared to *GRN*+ subjects. The fact that the *C9orf72*+ group showed atrophy that was not apparent in the *GRN*+ subjects is even more surprising given that the *C9orf72*+ subjects tended to be younger and farther from the mean age of disease onset in their families compared to the *GRN*+ subjects (13.7 versus 7.9 years, respectively). These findings suggest that the pathophysiology and early, preclinical course of disease associated with the *C9orf72* mutation differs from that associated with *GRN* mutations.

Previous studies of symptomatic *C9orf72*+ subjects have reported symmetric atrophy involving frontal, temporal, insular, and posterior cortical regions (Mahoney et al., 2012; Whitwell et al., 2012a; Sha et al., 2012; Boeve et al., 2012; Whitwell et al., 2013) and reduction in the subcortical volumes of thalamus, hippocampus (Floeter et al., 2016; Bede et al., 2013a; Scaber and Talbot, 2016; Westeneng et al., 2016; Westeneng et al., 2015; Omer et al., 2017). The GENFI study demonstrated similar diffuse brain atrophy in a combined group of symptomatic and asymptomatic *C9orf72*+ subjects (Rohrer et al., 2015). Using linear mixed effect models the GENFI study predicted cortical (frontal, temporal, parietal, occipital and cingulate) and subcortical (hippocampus, thalamus, striatum and amygdala) volume reduction to occur approximately 10–15 years prior to disease onset and 5–10 years earlier to decline in the performances of cognitive assessments. In a more recent analysis, they showed that presymptomatic gray matter atrophy was observed in the thalamus and cerebellum in the *C9orf72* group, and in the posterior frontal and parietal lobes as well as striatum in the *GRN* group, and in the anterior insula in both groups (Cash et al., 2018). In our study, we found similar patterns of structural changes including frontal (right postcentral, left rostral middle frontal and superior frontal gyri), temporal (right middle temporal, supra-marginal and superior temporal gyri), parietal regions (bilateral precuneus, right superior and inferior parietal gyri), thalamus and caudate in asymptomatic *C9orf72*+ subjects who were on average 13.7 years prior to disease onset. This finding is consistent with recent studies reporting loss of white matter integrity in tracks connecting to the frontal lobe and in the thalamic radiation in presymptomatic *C9orf72* carriers compared to controls (Papma et al., 2017). This is also consistent with functional connectivity studies demonstrating reduced white matter integrity in the corpus callosum, cingulum bundles, corticospinal tracts, uncinate

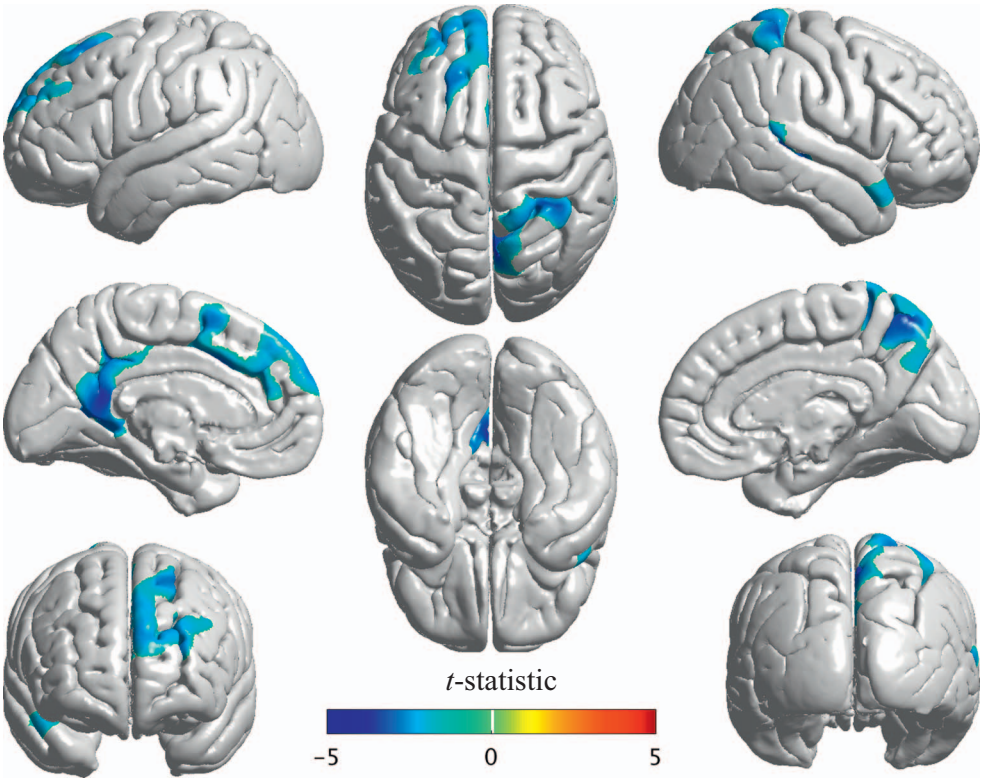

Fig. 1. Cortical thickness differences between *C9orf72+* ($n = 15$) compared to NC ($n = 37$). Illustration of the cortical regions with significant changes ($p < 0.05$) in thickness between *C9orf72+* and NC after correcting for the effects of age, sex and years to mean age of illness onset in family, controlled for multiple comparisons using cluster-based random field theory analysis.

Table 2
Cortical regions with significant reduction in thickness in *C9orf72+* as compared to NC.

Region	Number of vertices	*t*-Statistic[a]	*p***
Left rostral middle frontal gyrus	1858	−2.0637	0.0015
Left superior frontal gyrus	3822	−2.0809	0.0015
Left paracentral gyrus	124	−1.9593	0.0206
Caudal part of left anterior cingulate gyrus	64	−1.8682	0.0015
Isthmus of left cingulate gyrus	1026	−2.7203	0.0206
Left posterior cingulate gyrus	366	−1.9493	0.0206
Left lingual gyrus	112	−2.0628	0.0206
Left precuneus	1603	−2.422	0.0206
Right paracentral gyrus	105	−1.9318	0.0002
Right postcentral gyrus	120	−1.8401	0.0002
Right insular cortex	96	−1.8039	0.0126
Banks of right superior temporal sulcus	1062	−3.1283	0.0126
Right superior temporal gyrus	1968	−2.1678	0.0126
Right supra marginal gyrus	237	−1.9865	0.0002
Right middle temporal gyrus	397	−2.1385	0.0126
Right inferior parietal gyrus	520	−2.2106	0.0126
Right precuneus	1337	−2.1533	0.0002
Right superior parietal gyrus	3909	−2.1217	0.0002

[a] The median *t*-statistic in the significant cluster of vertices.

** *p*-values are controlled for multiple comparisons and corrected for sex, age and years to mean age of illness onset in the family.

fasciculi and inferior longitudinal fasciculi. Intrinsic connectivity deficits were most prominent in salience and medial pulvinar thalamus-seeded networks (Lee et al., 2017).

The structures we identified as being affected in our *C9orf72+* subjects correlate with the anatomy expected to be involved in causing the clinical and cognitive symptoms of FTD. Impairment in the cortical-subcortical neural circuits encompassing the right middle temporal gyrus, superior temporal gyrus, frontal gyrus, caudate and thalamus have been shown to be associated with executive dysfunction, apathy, disinhibition and deficits in social cognition, emotion recognition, and language (Bede et al., 2013a; Rosen et al., 2006; Rosen et al., 2005). In particular, the thalamus is known to play a crucial role in the relay and execution of several frontal lobe functions via the fronto-thalamic circuits and many previous studies have demonstrated involvement of the thalamus in *C9orf72+* subjects (Floeter et al., 2016; Bede et al., 2013a; Westeneng et al., 2015; Bede et al., 2013b), that may be relatively specific for this mutation (Sha et al., 2012). Cerebellar atrophy has also been described in affected *C9orf72+* patients, as it is now recognized that the cerebellum has integral function in cognitive and emotional processing (Bocchetta et al., 2016; Whitwell et al., 2012b; Irwin et al., 2013). However, we did not observe any significant cerebellar atrophy in our sample, likely because we were focusing on subjects at the pre-symptomatic phase, suggesting that cerebellar atrophy may occur at a later disease stage.

In contrast, previous studies of symptomatic *GRN+* subjects have reported a heterogeneous and asymmetric pattern of cortical atrophy (Mahoney et al., 2012; Whitwell et al., 2012a; Rohrer et al., 2010; Cruchaga et al., 2009; Rohrer et al., 2015). A recent study by Pievani et al. comparing five asymptomatic *GRN+* subjects with five *GRN−* subjects observed reduced cortical thickness (right lateral orbito-frontal cortex, left middle frontal gyrus and right precentral gyrus) (Pievani et al., 2014); however, these results were uncorrected, potentially leading to false positive changes. Cruchaga et al. also demonstrated gray matter changes in 4 *GRN+* subjects using voxel based morphometry analysis reporting uncorrected results, but the subjects were already showing early clinical symptoms on cognitive assessments (Cruchaga et al., 2009). Borroni et al. found no differences in gray matter volume between *GRN+* and *GRN−* (Borroni et al., 2008). Other groups have noted significant white matter changes in the periventricular subcortical white matter and U-fibers of *GRN+* carriers (Caroppo et al., 2014; Ameur et al., 2016). Using a rigorous cluster-based RFT method (Chung et al., 2010) (correcting for multiple comparisons) we did not find significant differences in cortical thickness or subcortical volumes among our asymptomatic *GRN+* subjects. It is possible that our negative result was due to the relatively small numbers in the *GRN+* cohort, which is a limitation of the current study. Alternatively, the pattern of atrophy among *GRN+* carriers may be too

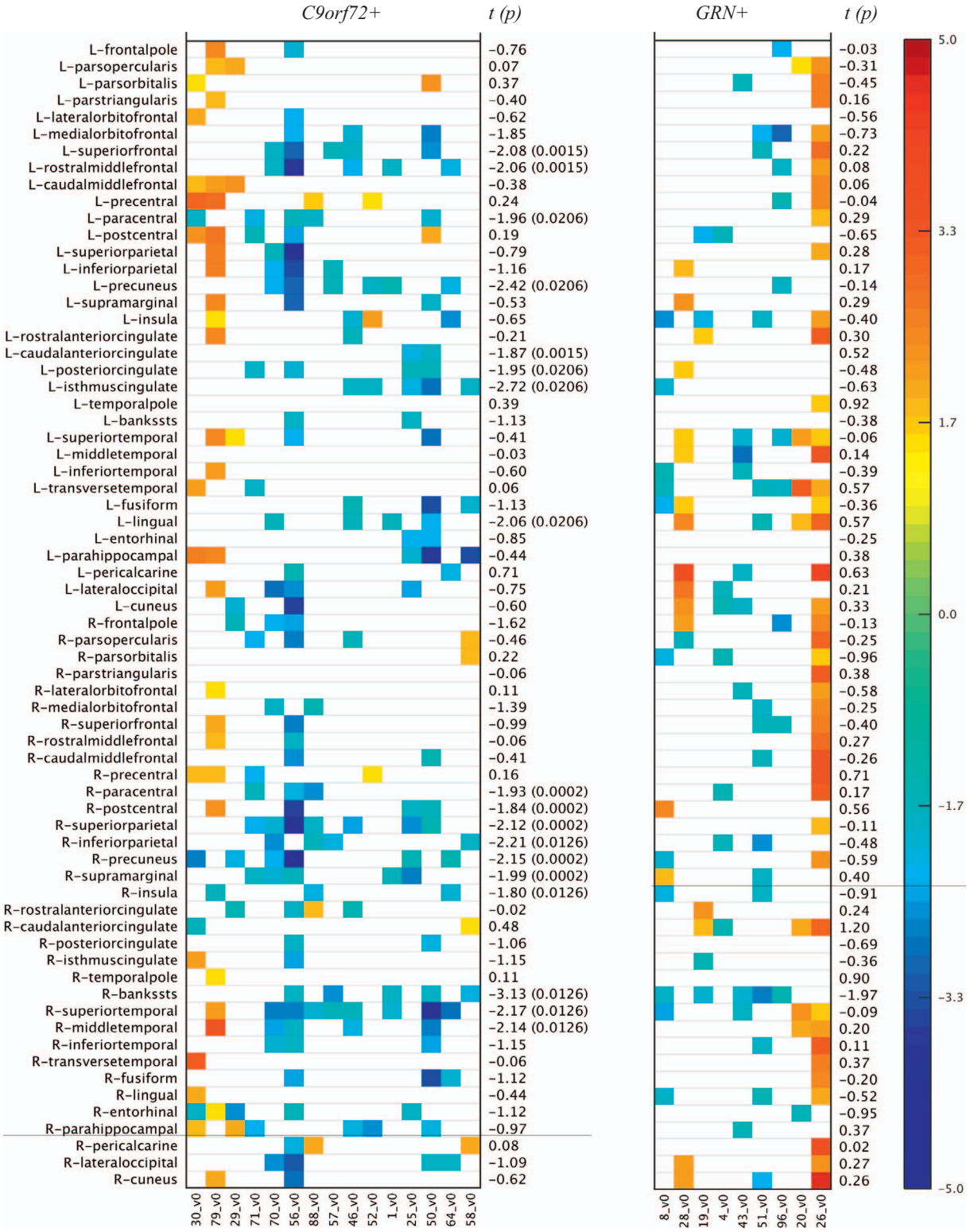

Fig. 2. Cortical thickness *z*-scores (age, sex and time to illness onset corrected) of subjects in the mutation carrier groups (*C9orf72+*, *GRN+*) sorted by age (youngest to oldest). The *z*-scores were computed by treating the NC group as the reference group. Only cases where $|z\text{-score}| > 1.5$ are shown. The *t*-statistic (*p*-value) corresponding to the mutation carriers versus the NC group differences are also given. The *p*-value is only reported for the significant (< 0.05) cases.

heterogeneous to be detectable in group-wise comparisons. Visual inspection of the significant differences across the gray matter regions (Figs. 2 and 3) suggest that indeed a few individuals may be having some early atrophy, but the changes are not severe enough and too variable to demonstrate statistical group differences.

Previous case series have discussed the heterogenous patterns of gray matter atrophy profile among symptomatic and asymptomatic *GRN+* (Whitwell et al., 2012b; Finch et al., 2009; Coppola et al., 2017; Beck et al., 2008). Furthermore, results from the GENFI study predicted that *GRN+* subjects would not show significant reduction in cortical volumes until approximately five years prior to illness onset, in which case, our *GRN+* subjects (on average eight years prior to predicted

Table 3
Subcortical volume measurements and comparison. The subcortical volumes for each subject were normalized with respect to their respective intracranial volume (ICV). The mean (std.) values (multiplied by factor of 10,000) are reported for each group. The *p*-values are controlled for multiple comparisons and corrected for the influences of sex, age and years to mean age of illness onset in the family. The bolded entries are the cases where the differences between the groups were statistically significant ($p < 0.05$).

	C9orf72+	*GRN+*	NC	*t*-Statistic (*p*)*	*t*-Statistic (*p*)**
Left thalamus	37.6 (5.2)	41.3 (4.7)	39.5 (4.8)	**−2.515 (0.015)**	0.202 (0.841)
Left caudate	18.5 (2.2)	18.6 (1.9)	18.9 (2.4)	**−2.243 (0.03)**	−0.662 (0.512)
Left putamen	29 (4)	28.9 (2.4)	27.9 (3.7)	−0.582 (0.563)	0.828 (0.412)
Left pallidum	8.3 (1.1)	8.2 (0.7)	8.1 (1.4)	−0.94 (0.352)	0.392 (0.697)
Left hippocampus	21.2 (2.5)	23.2 (1.7)	21.9 (2.3)	−1.956 (0.056)	0.848 (0.402)
Left amygdala	8.2 (1)	8.4 (1.6)	8.1 (0.8)	−0.406 (0.686)	0.633 (0.531)
Left accumbens	3.6 (0.5)	3.5 (0.6)	3.6 (0.7)	−0.864 (0.392)	−0.782 (0.438)
Right thalamus	34.9 (5)	36.8 (3.6)	36.3 (4.2)	**−3.042 (0.004)**	−0.689 (0.495)
Right caudate	19.2 (2)	18.9 (2.6)	19.3 (2.4)	−1.245 (0.219)	−0.245 (0.808)
Right putamen	26.6 (4)	28.4 (4.2)	26.5 (3.2)	−1.144 (0.258)	1.633 (0.110)
Right pallidum	8.2 (1.6)	8 (0.7)	7.9 (1.3)	−0.634 (0.529)	0.150 (0.882)
Right hippocampus	22.2 (2.2)	24.1 (2.1)	22.4 (2.3)	−1.263 (0.213)	1.313 (0.196)
Right amygdala	8.2 (1)	8.4 (1.3)	8.4 (1.1)	−0.829 (0.411)	−1.083 (0.285)
Right accumbens	3.7 (0.5)	3.7 (0.5)	3.6 (0.7)	−0.356 (0.723)	−0.425 (0.673)

* *C9orf72+* versus NC.
** *GRN+* versus NC.

onset) might still be too early to demonstrate significant atrophy. However, it is interesting that both GENFI and a previous study of ours found that *GRN+* subjects demonstrate cognitive and neuropsychological deficits as well as changes in glucose metabolism as early as 10 years prior to illness onset (Rohrer et al., 2015; Jacova et al., 2013; Hallam et al., 2014; Nasreddine et al., 2005); suggesting that the subtle decline in function precede obvious structural gray matter changes in the *GRN+* genetic subgroup. Finally, it is important to recognize that FTD represents a broad clinical spectrum with striking heterogeneity in the clinical features at the time of presentation, even among members of a family carrying a specific mutation. Whereas the non-motor manifestations in patients with the *C9orf72* mutation are most often behavioral or psychiatric, those with *GRN* mutations may present with bvFTD, PPA (usually the non-fluent variant), an Alzheimer's like amnestic syndrome, and less commonly corticobasal syndrome (Gass et al., 2006; Bang et al., 2015). Therefore, it is possible that this variation in the early clinical features of *GRN* mutation carriers is reflected by cortical involvement that is too variable in its focality and laterality to be evident in a group-wise analysis. If this is the case, then an alternative method of analysis would be necessary to appreciate the early changes within this genetic subgroup (e.g. non-biased measure of the presence of any significant asymmetry or focal change, regardless of anatomic location).

There are certain limitations to our current study, which include the relatively small sample size, cross-sectional design, limited MRI measures and neuropsychological data. Future studies should include longitudinal assessments, white matter measures, and correlation with detailed neuropsychological data.

5. Conclusion

Despite the limitations, our study suggest that the patterns of early cerebral atrophy differ between *C9orf72* and *GRN* mutation carriers, suggesting potentially important difference in the pathogenic pathways between the two subtypes of FTD. While longitudinal follow up with an augmented sample size and multimodal imaging are needed to confirm these findings, our current data suggest that structural imaging does have utility as a biomarker of early disease, and the pattern may depend on the specific genetic factors involved in the patient population being studied.

Acknowledgements

The authors would like to thank all the participants of the research study. The study is supported by funding from the Canadian Institutes of Health Research operating grant #179009 and #74580, the Pacific

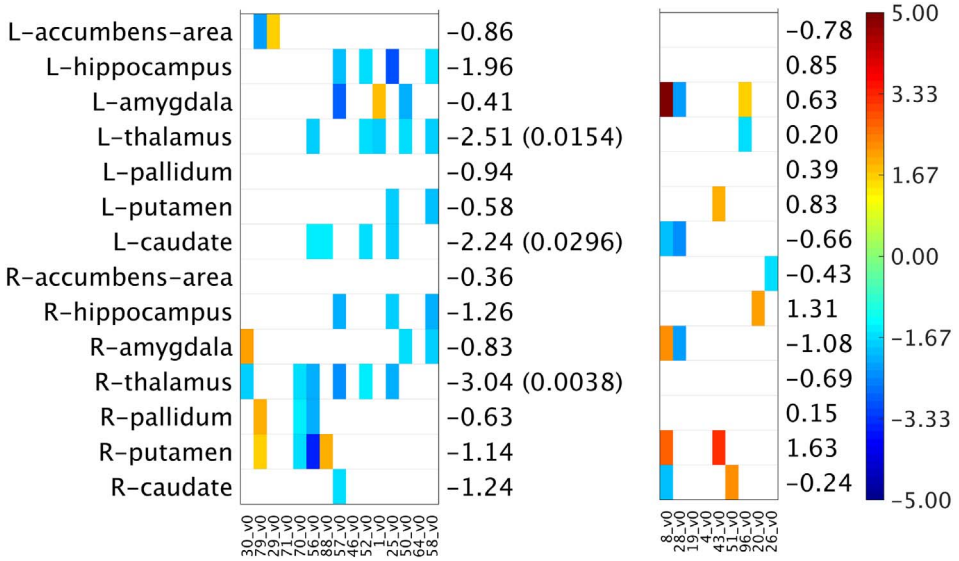

Fig. 3. Subcortical volumes *z*-scores (age, sex and time to illness onset corrected) of subjects in the mutation carrier groups (*C9orf72+*, *GRN+*) sorted by age (youngest to oldest). The *z*-scores were computed by treating the NC group as the reference group. Only cases where $|z\text{-score}| > 1.5$ are shown. Blue represents a negative z-score, which implies a reduced subcortical volume in a *C9orf72+/GRN+* subject relative to the "mean" subcortical volume estimated from the subjects in the reference NC group. Whereas, a red point means a positive z-score, which implies an increased subcortical volume in a *C9orf72+/GRN+* subject relative to the "mean" subcortical volume in the NC group. The *t*-statistic (*p*-value) corresponding to the mutation carriers (*C9orf72+*, *GRN+*) versus the NC group differences are also given. The *p*-value is only reported for the significant (< 0.05) cases. (For interpretation of the references to color in this figure legend, the reader is referred to the web version of this article.)

Alzheimer's Research Foundation (PARF center grant C06-01), and the National Institutes of Health R01 NS065782 to Rosa Rademakers and R01 AG055121-01A1 in support of research on frontotemporal dementia. Dr. Hsiung is supported by funding through the Ralph Fisher Professorship in Alzheimer's Research (Alzheimer Society of British Columbia, Canada) and by a CIHR Clinical Genetics Investigatorship award. Drs. Beg, Popuri and Balachandar are supported by funding from NSERC, Alzheimer's society Research program, PARF, Genome BC and Brain Canada.

Appendix A. Supplementary data

Supplementary data to this article can be found online at https://doi.org/10.1016/j.nicl.2018.02.017.

References

Ameur, F., Colliot, O., Caroppo, P., et al., 2016. White matter lesions in FTLD: distinct phenotypes characterize *GRN* and *C9ORF72* mutations. Neurol. Genet. 2 (1), e47. (cited 2018 Jan 15) Available from: https://doi.org/10.1212/NXG.0000000000000047.

Baker, M., Mackenzie, I.R., Pickering-Brown, S.M., et al., 2006. Mutations in progranulin cause tau-negative frontotemporal dementia linked to chromosome 17. Nature 442 (7105), 916–919. Available from: http://www.ncbi.nlm.nih.gov/pubmed/16862116.

Bang, J., Spina, S., Miller, B.L., 2015. Non-Alzheimer's dementia 1 Frontotemporal dementia. Lancet 386, 1672–1682.

Beck, J., Rohrer, J.D., Campbell, T., et al., 2008. A distinct clinical, neuropsychological and radiological phenotype is associated with progranulin gene mutations in a large UK series. Brain 131 (Pt 3), 706–720. (cited 2017 Nov 8) Available from: http://www.ncbi.nlm.nih.gov/pubmed/18234697.

Bede, P., Elamin, M., Byrne, S., et al., 2013a. Basal ganglia involvement in amyotrophic lateral sclerosis. Neurology 81 (24), 2107–2115.

Bede, P., Bokde, A.L.W., Byrne, S., et al., 2013b. Multiparametric MRI study of ALS stratified for the C9orf72 genotype. Neurology 81 (4), 361–369.

Beg, M.F., Miller, M.I., Trouvé, A., Younes, L., 2005. Computing large deformation metric mappings via geodesic flows of diffeomorphisms. Int. J. Comput. Vis. 61 (2), 139–157.

Bocchetta, M., Cardoso, M.J., Cash, D.M., et al., 2016. Patterns of regional cerebellar atrophy in genetic frontotemporal dementia. NeuroImage Clin. 11, 287–290.

Boeve, B.F., Boylan, K.B., Graff-Radford, N.R., et al., 2012. Characterization of frontotemporal dementia and/or amyotrophic lateral sclerosis associated with the GGGGCC repeat expansion in C9ORF72. Brain 135 (3), 765–783. Available from: https://doi.org/10.1093/brain/aws004.

Borroni, B., Alberici, A., Premi, E., et al., 2008. Brain magnetic resonance imaging structural changes in a pedigree of asymptomatic progranulin mutation carriers. Rejuvenation Res. 11 (3), 585–595. Available from: https://doi.org/10.1089/rej.2007.0623.

Boxer, A.L., Mackenzie, I.R., Boeve, B.F., et al., 2011. Clinical, neuroimaging and neuropathological features of a new chromosome 9p-linked FTD-ALS family. J. Neurol. Neurosurg. Psychiatry 82 (2), 196–203. Available from: https://doi.org/10.1136/jnnp.2009.204081.

Brooks, B.R., Miller, R.G., Swash, M., et al., 2000. El Escorial revisited: revised criteria for the diagnosis of amyotrophic lateral sclerosis. Amyotroph. Lateral Scler. Other Motor Neuron Disord. 1 (5), 293–299.

Caroppo, P., Le Ber, I., Camuzat, A., et al., 2014. Extensive white matter involvement in patients with frontotemporal lobar degeneration. JAMA Neurol. 71 (12), 1562. (cited 2018 Jan 15) Available from: http://www.ncbi.nlm.nih.gov/pubmed/25317628.

Cash, D.M., Bocchetta, M., Thomas, D.L., et al., 2018. Patterns of gray matter atrophy in genetic frontotemporal dementia: results from the GENFI study. Neurobiol. Aging 62, 191–196. (cited 2018 Jan 15) Available from: http://www.ncbi.nlm.nih.gov/pubmed/29172163.

Chung, M.K., Worsley, K.J., Nacewicz, B.M., et al., 2010. General multivariate linear modeling of surface shapes using SurfStat. NeuroImage 53 (2), 491–505. Available from: http://linkinghub.elsevier.com/retrieve/pii/S1053811910008761.

Coppola, C., Saracino, D., Puoti, G., et al., 2017. A cluster of progranulin C157KfsX97 mutations in Southern Italy: clinical characterization and genetic correlations. Neurobiol. Aging 49, 219.e5–219.e13. (cited 2017 Nov 8) Available from: http://www.ncbi.nlm.nih.gov/pubmed/27814992.

Cruchaga, C., Fernandez-Seara, M.A., Seijo-Martinez, M., et al., 2009. Cortical atrophy and language network reorganization associated with a novel Progranulin mutation. Cereb. Cortex 19 (8), 1751–1760. Available from: https://doi.org/10.1093/cercor/bhn202.

Cruts, M., Gijselinck, I., van der Zee, J., et al., 2006. Null mutations in progranulin cause ubiquitin-positive frontotemporal dementia linked to chromosome 17q21. Nature 442 (7105), 920–924. Available from: http://www.ncbi.nlm.nih.gov/pubmed/16862115.

Dale, A.M., Fischl, B., Sereno, M.I., 1999. Cortical surface-based analysis. I. Segmentation and surface reconstruction. NeuroImage 9 (2), 179–194. Available from: http://www.ncbi.nlm.nih.gov/pubmed/9931268.

DeJesus-Hernandez, M., Mackenzie, I.R., Boeve, B.F., et al., 2011. Expanded GGGGCC hexanucleotide repeat in noncoding region of C9ORF72 causes chromosome 9p-linked FTD and ALS. Neuron 72 (2), 245–256. Available from: http://www.ncbi.nlm.nih.gov/pubmed/21944778.

Diedrichsen, J., Balster, J.H., Flavell, J., Cussans, E., Ramnani, N., 2009. A probabilistic MR atlas of the human cerebellum. Neuroimage.

Diedrichsen, J., Maderwald, S., Küper, M., Thürling, M., Rabe, K., Gizewski, E.R., Ladd, M., Timmann, D., 2011. Imaging the deep cerebellar nuclei: A probabilistic atlas and normalization procedure. Neuroimage.

Dubois, B., Slachevsky, A., Litvan, I., Pillon, B., 2000. The FAB: a frontal assessment battery at bedside. Neurology 55 (11), 1621–1626.

Feldman, H., Levy, A.R., Hsiung, G.-Y., et al., 2003. A Canadian cohort study of cognitive impairment and related dementias (ACCORD): study methods and baseline results. Neuroepidemiology 22 (5), 265–274. Available from: http://www.ncbi.nlm.nih.gov/pubmed/12902621.

Finch, N., Baker, M., Crook, R., et al., 2009. Plasma progranulin levels predict progranulin mutation status in frontotemporal dementia patients and asymptomatic family members. Brain 132 (Pt 3), 583–591. (cited 2017 Nov 8) Available from: http://www.ncbi.nlm.nih.gov/pubmed/19158106.

Fischl, B., Dale, A.M., 2000. Measuring the thickness of the human cerebral cortex from magnetic resonance images. Proc. Natl. Acad. Sci. U. S. A. 97 (20), 11050–11055. Available from: https://doi.org/10.1073/pnas.200033797.

Fischl, B., Sereno, M.I., Dale, A.M., 1999. Cortical surface-based analysis - II: inflation, flattening, and a surface-based coordinate system. NeuroImage 9 (2), 195–207.

Fischl, B., Salat, D.H., Busa, E., et al., 2002. Whole brain segmentation: automated labeling of neuroanatomical structures in the human brain. Neuron 33 (3), 341–355. Available from: http://www.ncbi.nlm.nih.gov/entrez/query.fcgi?cmd=Retrieve&db=PubMed&dopt=Citation&list_uids=11832223.

Floeter, M.K., Bageac, D., Danielian, L.E., et al., 2016. Longitudinal imaging in C9orf72 mutation carriers: relationship to phenotype. NeuroImage Clin. 12, 1035–1043.

Folstein, M.F., Folstein, S.E., McHugh, P.R., 1975. Mini-mental state. J. Psychiatr. Res. 12 (3), 189–198.

Folstein, M.F., Robins, L.N., Helzer, J.E., 1983. The mini-mental state examination. Arch. Gen. Psychiatry 40 (7), 812.

Gass, J., Cannon, A., Mackenzie, I.R., et al., 2006. Mutations in progranulin are a major cause of ubiquitin-positive frontotemporal lobar degeneration. Hum. Mol. Genet. 15 (20), 2988–3001.

Gijselinck, I., Van Langenhove, T., van der Zee, J., et al., 2012. A C9orf72 promoter repeat expansion in a Flanders-Belgian cohort with disorders of the frontotemporal lobar degeneration-amyotrophic lateral sclerosis spectrum: a gene identification study. Lancet Neurol. 11 (1), 54–65.

Gorno-Tempini, M.L., Hillis, A.E., Weintraub, S., et al., 2011. Classification of primary progressive aphasia and its variants. Neurology 76 (11), 1006–1014.

Grabner, G., Janke, A.L., Budge, M.M., et al., 2006. Symmetric atlasing and model based segmentation: an application to the hippocampus in older adults. Med. Image Comput. Comput. Assist. Interv. 9 (Pt 2), 58–66. Available from: http://www.ncbi.nlm.nih.gov/pubmed/17354756.

Hallam, B.J., Jacova, C., G-YR, Hsiung, et al., 2014. Early neuropsychological characteristics of progranulin mutation carriers. J. Int. Neuropsychol. Soc. 20 (7), 694–703. Available from: http://www.journals.cambridge.org/abstract_S1355617714000551.

Irwin, D.J., McMillan, C.T., Brettschneider, J., et al., 2013. Cognitive decline and reduced survival in *C9orf72* expansion frontotemporal degeneration and amyotrophic lateral sclerosis. J. Neurol. Neurosurg. Psychiatry 84 (2), 163–169. (cited 2018 Jan 24) Available from: http://www.ncbi.nlm.nih.gov/pubmed/23117491.

Jacova, C., Hsiung, G.-Y.R., Tawankanjanachot, I., et al., 2013. Anterior brain glucose hypometabolism predates dementia in progranulin mutation carriers. Neurology 81 (15), 1322–1331. Available from: https://doi.org/10.1212/WNL.0b013e3182a8237e.

Kertesz, A., Nadkarni, N., Davidson, W., Thomas, A.W., 2000. The Frontal Behavioral Inventory in the differential diagnosis of frontotemporal dementia. J. Int. Neuropsychol. Soc. 6 (4), 460–468. (cited 2018 Jan 15) Available from: http://www.ncbi.nlm.nih.gov/pubmed/10902415.

Lee, S.E., Sias, A.C., Mandelli, M.L., et al., 2017. Network degeneration and dysfunction in presymptomatic C9ORF72 expansion carriers. NeuroImage Clin. 14, 286–297. (cited 2018 Jan 15) Available from: http://www.ncbi.nlm.nih.gov/pubmed/28337409.

Mahoney, C.J., Beck, J., Rohrer, J.D., et al., 2012. Frontotemporal dementia with the C9ORF72 hexanucleotide repeat expansion: clinical, neuroanatomical and neuropathological features. Brain 135 (3), 736–750. Available from: https://doi.org/10.1093/brain/awr361.

McKhann, G.M., Albert, M.S., Grossman, M., et al., 2001. Clinical and pathological diagnosis of frontotemporal dementia: report of the Work Group on Frontotemporal Dementia and Pick's disease. Arch. Neurol. 58 (11), 1803–1809. Available from: http://www.ncbi.nlm.nih.gov/pubmed/11708987.

Nasreddine, Z.S., Phillips, N.A., BÃ©Dirian, V., et al., 2005. The Montreal cognitive assessment, MoCA: a brief screening tool for mild cognitive impairment. J. Am. Geriatr. Soc. 53 (4), 695–699.

Omer, T., Finegan, E., Hutchinson, S., et al., 2017. Neuroimaging patterns along the ALS-FTD spectrum: a multiparametric imaging study. Amyotroph. Lateral Scler. Front. Degener. 18 (7–8), 611–623. (cited 2018 Jan 24) Available from: http://www.ncbi.nlm.nih.gov/pubmed/28562080.

Pan, X.-D., Chen, X.-C., 2013. Clinic, neuropathology and molecular genetics of frontotemporal dementia: a mini-review. Transl. Neurodegener. 2 (1), 8.

Papma, J.M., Jiskoot, L.C., Panman, J.L., et al., 2017. Cognition and gray and white matter characteristics of presymptomatic *C9orf72* repeat expansion. Neurology 89 (12), 1256–1264. (cited 2018 Jan 15) Available from: http://www.ncbi.nlm.nih.

gov/pubmed/28855404.
Pievani, M., Paternicò, D., Benussi, L., et al., 2014. Pattern of structural and functional brain abnormalities in asymptomatic granulin mutation carriers. Alzheimers Dement. 10((5), S354–S363.e1.
Rascovsky, K., Hodges, J.R., Knopman, D., et al., 2011. Sensitivity of revised diagnostic criteria for the behavioural variant of frontotemporal dementia. Brain 134 (Pt 9), 2456–2477.
Renton, A.E., Majounie, E., Waite, A., et al., 2011. A hexanucleotide repeat expansion in C9ORF72 is the cause of chromosome 9p21-linked ALS-FTD. Neuron 72 (2), 257–268.
Rohrer, J.D., Ridgway, G.R., Modat, M., et al., 2010. Distinct profiles of brain atrophy in frontotemporal lobar degeneration caused by progranulin and tau mutations. NeuroImage 53 (3), 1070–1076. Available from: http://linkinghub.elsevier.com/retrieve/pii/S1053811909013779.
Rohrer, J.D., Nicholas, J.M., Cash, D.M., et al., 2015. Presymptomatic cognitive and neuroanatomical changes in genetic frontotemporal dementia in the genetic frontotemporal dementia initiative (GENFI) study: a cross-sectional analysis. Lancet Neurol. 14 (3), 253–262. Available from: http://linkinghub.elsevier.com/retrieve/pii/S1474442214703242.
Rosen, H.J., Allison, S.C., Schauer, G.F., et al., 2005. Neuroanatomical correlates of behavioural disorders in dementia. Brain 128 (Pt 11), 2612–2625. Available from: http://www.ncbi.nlm.nih.gov/pubmed/16195246.
Rosen, H.J., Wilson, M.R., Schauer, G.F., et al., 2006. Neuroanatomical correlates of impaired recognition of emotion in dementia. Neuropsychologia 44 (3), 365–373. Available from: http://www.ncbi.nlm.nih.gov/pubmed/16154603.
Scaber, J., Talbot, K., 2016. What is the role of TDP-43 in *C9orf72*-related amyotrophic lateral sclerosis and frontemporal dementia? Brain 139 (12), 3057–3059.
Seelaar, H., Kamphorst, W., Rosso, S.M., et al., 2008. Distinct genetic forms of frontotemporal dementia. Neurology 71 (16), 1220–1226. Available from: https://doi.org/10.1212/01.wnl.0000319702.37497.72.
Sha, S.J., Takada, L.T., Rankin, K.P., et al., 2012. Frontotemporal dementia due to C9ORF72 mutations: clinical and imaging features. Neurology 79 (10), 1002–1011. Available from: https://doi.org/10.1212/WNL.0b013e318268452e.
Snowden, J.S., Neary, D., Mann, D.M.A., 2002. Frontotemporal dementia. Br. J. Psychiatry 180, 140–143. Available from: http://www.ncbi.nlm.nih.gov/pubmed/11823324.
Snowden, J.S., Neary, D., Mann, D.M.A., et al., 2005. Frontotemporal dementia. Lancet Neurol. 4 (11), 771–780. Available from: http://linkinghub.elsevier.com/retrieve/pii/S1474442205702234.
Warren, J.D., Rohrer, J.D., Rossor, M.N., 2013. Frontotemporal dementia. BMJ 347.
Westeneng, H.-J., Verstraete, E., Walhout, R., et al., 2015. Subcortical structures in amyotrophic lateral sclerosis. Neurobiol. Aging 36 (2), 1075–1082.
Westeneng, H.-J., Walhout, R., Straathof, M., et al., 2016. Widespread structural brain involvement in ALS is not limited to the C9orf72 repeat expansion. J. Neurol. Neurosurg. Psychiatry 87 (12), 1354–1360.
Whitwell, J.L., Jack, C.R., Boeve, B.F., et al., 2009. Voxel-based morphometry patterns of atrophy in FTLD with mutations in MAPT or PGRN. Neurology 72 (9), 813–820. Available from: http://www.ncbi.nlm.nih.gov/pubmed/19255408.
Whitwell, J.L., Weigand, S.D., Boeve, B.F., et al., 2012a. Neuroimaging signatures of frontotemporal dementia genetics: C9ORF72, tau, progranulin and sporadics. Brain 135 (3), 794–806. Available from: doi/10.1093/brain/aws001 (cited 2017 Nov 5).
Whitwell, J.L., Weigand, S.D., Boeve, B.F., et al., 2012b. Neuroimaging signatures of frontotemporal dementia genetics: C9ORF72, tau, progranulin and sporadics. Brain 135 (Pt 3), 794–806. Available from: http://www.ncbi.nlm.nih.gov/pubmed/22366795.
Whitwell, J.L., Xu, J., Mandrekar, J., et al., 2013. Frontal asymmetry in behavioral variant frontotemporal dementia: clinicoimaging and pathogenetic correlates. Neurobiol. Aging 34 (2), 636–639. Available from: http://www.ncbi.nlm.nih.gov/pubmed/22502999.